MODELLING ROUGHNESS CHANGE DUE TO BED FORM GROWTH UNDER TRANSIENT FLOWS

William Bonino Rauen [1]; *Vinícius Granadier* [2]

ABSTRACT – This study focused on the modelling capacity of unsteady resistance coefficients for hydraulic models. The specific aim was to adapt and test a calculation procedure for coefficient variation governed by roughness change due to bed form development under transient flow. An established method so far only used successfully under steady flow conditions was analysed through the lens of unsteady flow, adapted and used to simulate ripple growth in a wide channel reach with sand bed, with a triangular flow hydrograph as passing flood wave. The corresponding effects on water depth predictions were also contrasted with their counterparts obtained using a temporally constant resistance coefficient normally associated with equilibrium bed forms. Due to its highly parameterised nature, the new procedure can potentially contribute to improve modelling performance, cost-effectively, in such type of challenging simulation conditions.

Palavras-Chave – modelagem; rugosidade; transiente.

1 - INTRODUCTION

Hydraulic models for open channel flows with sediment transport often represent flow resistance through coefficients such as Manning's *n* or Chezy's *C*, with the values of which often being determined through calibration using field or laboratory data (e.g. for water levels). Such boundary condition can be steady and uniform, particularly for quasi-steady and quasi-uniform flows. On occasions, reference values for a given resistance coefficient are associated with the type of bed form occurring or thought to occur on a modelled alluvial bed (e.g. Brunner, 2010), thus reflecting the key role played by the bed roughness in establishing overall resistance to flow. In this sense, a further development is to compute a given coefficient as a function of bed form dimensions, such as representative height η and length λ values (e.g. Deltares, 2014; Brunner, 2016), which can depend heavily on the flow condition (van Rijn, 2007). This type of approach allows for automatic calculation of spatial and temporal variation of coefficient values in a

1) Professor Adjunto, Departamento de Hidráulica e Saneamento (DHS) e Programa de Pós-Graduação em Engenharia de Recursos Hídricos e Ambiental (PPGERHA), Universidade Federal do Paraná (UFPR). Email: wbrauen@gmail.com.
2) Mestrando e bolsista CAPES no Programa de Pós-Graduação em Engenharia de Recursos Hídricos e Ambiental (PPGERHA), Universidade Federal do Paraná (UFPR). Email: viniciusgranadier@gmail.com.

computational domain and simulation timeframe, grounded on knowledge and mathematical description of the physics of two-way interactions between flow hydrodynamics and morphological features. Such flow-coupled representation of the lower boundary condition can benefit modelling performance particularly for transient flows, such as caused by flood or tidal waves, over fields of mega-ripples and/or dunes – the dimensions of which are affected by the flow depth.

It is noteworthy, however, that equilibrium stage dimensions η_e and λ_e are typically used in the latter context without verification of their occurrence (even theoretically) in a given simulation. As the amount of time required to reach equilibrium (t_e) can vary from a few hours to several days, bed form dimensions may never reach their equilibrium levels in a simulation timeframe, depending on the rate of change of transient flow, sediment characteristics and the pre-existing bed state – instead, η and λ may constantly fluctuate between successive non-equilibrium values. Such unsteadiness of the bed roughness condition can be described using more or less parameterised approaches (Coleman et al., 2005; Paarlberg et al., 2009; Warmink et al., 2015) which are, nonetheless, not yet part of standard hydraulic modelling practice. This is partly due to limited availability of field and laboratory bed morphology data obtained under transient flow conditions, and an incomplete understanding and descriptive ability of related processes.

In the case of bed form development (growth) from a plane bed, equation (1) (Coleman et al., 2005) can be used to estimate η and λ as a function of time under a steady flow regime. Figure 1a illustrates the power curves obtained using equation (1) for the normalised dimensions as a function of normalised time, where normalisation of η, λ and t values is achieved by division by the corresponding equilibrium values (η_e, λ_e and t_e, respectively, which are constant under steady flow). Formulae to calculate the growth exponents γ_η and γ_λ for such power curves and to estimate t_e for ripples and dunes can also be found in Coleman et al. (2005).

$$\frac{\eta}{\eta_e} = \left(\frac{t}{t_e}\right)^{\gamma_\eta} \quad \text{and} \quad \frac{\lambda}{\lambda_e} = \left(\frac{t}{t_e}\right)^{\gamma_\lambda} \tag{1}$$

It can be noted in Figure 1b that the growth rate decreases as a bed form dimension approaches its equilibrium level, as the amount of growth over a given period of time depends upon the instantaneous condition. Under transient flow, such as caused by a passing flood wave through a channel reach, bed form development can be reasonably assumed to follow a similar pattern. Hence, the amount of bed form growth over, say, a hydrograph flow step of duration Δt would thus depend on the dimensions in the beginning of such time step (η_i, λ_i). However, thus far, bed form development under transient flows does not appear to have been adequately parameterised using relatively simple formulae as equation (1). For instance, Warmink et al.

(2015) had to resort to a more complex and computationally expensive hydro-morphodynamic approach to achieve a realistic description of bed form growth and its effects on flow parameters. Their results obtained using equation (1) in its standard steady flow form show that it was unsuitable for their transient flow simulations.

As part of the conceptual basis for the present paper, further analysis of equation (1) showed that it may be used to describe bed form development also under transient flows, provided that the meaning of each term is also viewed through the lens of transient flow. Hence, the aim of this study was to develop and test a new procedure to compute bed form growth under transient flow, based on Coleman et al. (2005)'s equation so far only used for steady flows.

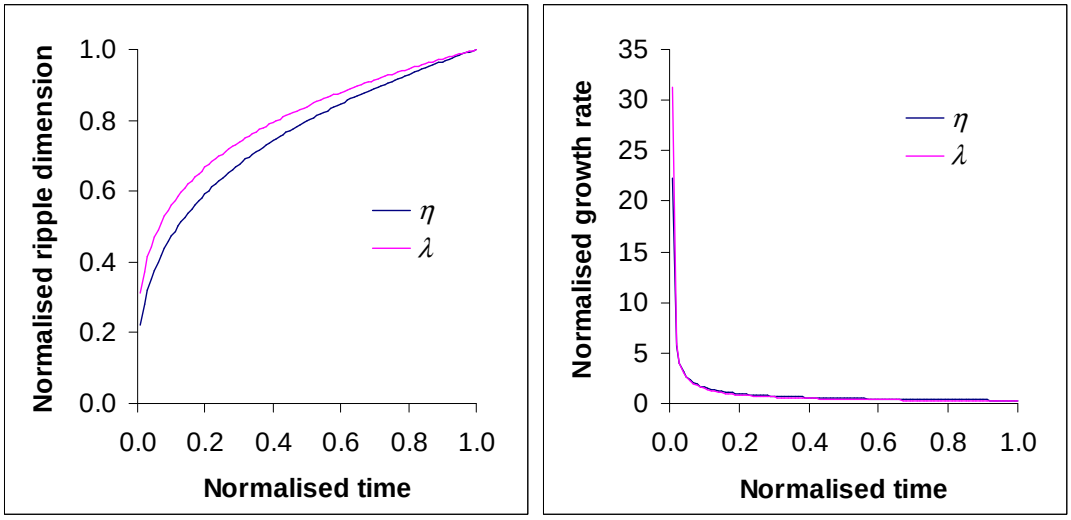

Figure 1 – Time variation of (a) normalised ripple dimensions and (b) normalised growth rates for ripple height (η) and length (λ).

2 - METHODS

An analysis of equation (1) through the lens of bed form development under transient flows revealed that treating t_e as constant throughout an unsteady flow simulation would be unrealistic, as t_e is a function of the flow condition (e.g. equation 2 below) – in general, stronger flows accelerate development and, thus, reduce the amount of time required to reach the equilibrium stage. Thus, t_e requires updating in each new flow step, being understood as the time required to reach equilibrium dimensions if the flow remained in such an instantaneous condition long enough – which can be interpreted as a hypothetical equilibrium condition.

Similarly, η_e and λ_e should be associated with such a hypothetical equilibrium condition and require updating at each new flow step, in the case of mega-ripples and dunes (terminology in line with the bed form classification scheme of van Rijn, 2007). For mini-ripples with equilibrium dimensions depending only on the grain size, η_e and λ_e do not require updating.

The time stamp t should not simply be made equal to Δt in each new flow step, as this would cause growth rates to be overestimated (as if bed forms were always in the beginning of their development history, see Figure 1b). On the other hand, equating t to the absolute hydrograph time (T) while updating t_e, η_e and λ_e as mentioned above would cause a mismatch in the parameter base and unrealistic discontinuities in the development curves. Thus, t should represent, at each flow step, the bed form growth history as described by Figure 1a, which does not necessarily match T in transient flow cases. Such decoupling of time stamps is the essence of the procedure outlined below, which has allowed for adapting Coleman et al. (2005)'s method (equation 1) developed for steady flow conditions for usage also in transient flow simulations involving bed form development.

2.1 - Calculation procedure for $\eta(t)$ and $\lambda(t)$ under a transient flow regime

The procedure starts by calculating or assigning values of parameters that are assumed not to depend on the flow condition, such as γ_η and γ_λ. In the case of mini-ripples, η_e and λ_e can be calculated only once following Raudkivi (1997) (in mm): $\eta_e = 18.16d^{0.097}$ and $\lambda_e = 245d^{0.35}$. For mega-ripples and dunes, the corresponding η_e and λ_e values require updating at each new flow step using other established formulae, such as found in van Rijn (2007).

Then, for each flow step (duration Δt) used to discretise the flood wave hydrograph, assume occurrence of a quasi-steady and quasi-uniform flow regime and calculate t_e using available formulae for the type of bed form. For example, for mini-ripples (Coleman et al., 2005):

$$t_e = \frac{d}{u_{*e}} 2{,}08x10^8 \left(\frac{\theta_e}{\theta_c}\right)^{-2{,}42} \qquad (2)$$

where, in line with Coleman et al. (2005), u_{*e} and θ_e are the total (non-partitioned) shear velocity and Shields parameter, respectively, of such hypothetical equilibrium condition (separate procedure, see section 2.2). It is noteworthy that equation (2) was obtained by Coleman et al. (2005) using regression analysis of the equilibrium values of parameters used to characterise the set of bed form development experiments thus considered. This explains why it is necessary to estimate parameters for such an equilibrium condition even if it is never verified in practice – each hypothetical equilibrium condition associated with successive flow steps serves only as the instantaneous ultimate target of bed form development, which influences the instantaneous rate of development according to the pattern defined by equation (1) and Figure 1b.

Then, solve equation (3), which is obtained from equation (1) with $t_i = t$, $\eta_i = \eta$ and $\lambda_i = \lambda$.

$$t_i = \left(\frac{\eta_i}{\eta_e}\right)^{\gamma_\eta^{-1}} t_e \quad \text{or} \quad t_i = \left(\frac{\lambda_i}{\lambda_e}\right)^{\gamma_\lambda^{-1}} t_e \qquad (3)$$

where the values of ripple height and length occurring in the beginning of a flow step, i.e. η_i and λ_i, are equated to the corresponding values occurring in the end of the previous flow step. Each t_i value obtained using equation (3) is a time stamp associated with the beginning of a flow step, as if all bed form development up to that moment had occurred under such flow condition.

Then, calculate the time stamp associated with the end of a flow step, as $t_f = t_i + \Delta t$, and solve equation (4) – also obtained from equation (1) – for η_f and λ_f, as:

$$\eta_f = \eta_e \left(\frac{t_f}{t_e} \right)^{\gamma_\eta} \quad \text{and} \quad \lambda_f = \lambda_e \left(\frac{t_f}{t_e} \right)^{\gamma_\lambda} \tag{4}$$

Finally, record the η_f and λ_f values as part of the time series $\eta(t)$ and $\lambda(t)$ and repeat the previous steps until an equilibrium condition is reached or the end of the simulation period. The growth history is represented by the time series of $\eta(t)$ and $\lambda(t)$ values, each varying from zero (plane bed) to the corresponding equilibrium dimensions η_e and λ_e.

2.2 - Calculation procedure for u_{*e} and θ_e

Parameters u_{*e} and θ_e are the total (non-partitioned) shear velocity and Shields number, respectively, of the hypothetical equilibrium state. Assuming a quasi-steady and quasi-uniform flow regime in each flow step, u_{*e} can be estimated using the general flow resistance equation as:

$$u_{*e} = \sqrt{g h_e I_0} \tag{5}$$

where g is the acceleration due to gravity, I_0 is the channel slope and h_e is the hypothetical equilibrium water depth, calculated using Manning's equation as:

$$h_e = \left(\frac{q n_e}{I_0^{0,5}} \right)^{\frac{3}{5}} \tag{6}$$

where q is the specific discharge and n_e is the hypothetical equilibrium Manning coefficient, calculated using Strickler's equation as:

$$n_e = \frac{k_{se}^{1/6}}{26} \tag{7}$$

where k_{se} is the hypothetical equilibrium Nikuradse roughness coefficient, calculated using the roughness partitioning equation as $k_{se} = k_{ss} + k_{sfe}$, where $k_{ss} = 3d_{90}$ is the skin friction component, with d_{90} being the 90th percentile of sediment grain size distribution curve. The form drag component in the hypothetical equilibrium state (k_{sfe}) can be calculated as (for mini-ripples):

$$k_{sfe} = \alpha \frac{\eta_e^2}{\lambda_e} \tag{8}$$

where $\alpha = 30$ following Soulsby (1997).

The corresponding value of the Shields number for such hypothetical equilibrium state can be calculated as:

$$\theta_e = \frac{u_{*e}^2}{gd(S_s - 1)} \tag{9}$$

where d and S_s are the sediment median particle size and specific gravity, respectively.

2.3 - Test conditions

Application of the modelling procedure is demonstrated for the case of ripple development in a hypothetical channel reach with passing flood wave. Simulations were conducted using spreadsheet software. A mixture of fine and medium silica sand (S_s = 2.65, d = 0.235 mm, d_{90} = 0.327 mm) was assumed as channel bed, which gave the normalised grain size value D_* = 5.94 and critical Shields number θ_c = 0.045. Based on Coleman et al. (2005), γ_η = 0.33 and γ_λ = 0.25 were exponents for the ripple height and length growth curves, respectively. Based on Raudkivi (1997), η_e = 15.8 mm and λ_e = 148 mm, so that k_{sfe} = 50.6 mm (equation 8), k_{se} = 51.6 mm and n_e = 0.0235 (equation 7). The channel slope I_0 = 0.00005 m/m was determined by trial and error to give wide channel flow with bedload sediment transport occurring throughout the simulation.

The flood wave consisted of a triangular hydrograph with base flow q_b = 0.11 m^3/sm, peak flow q_p = 0.53 m^3/sm, base time t_b = 72 hr and peak time t_p = 24 hr. The simulation time step was Δt = 1 hr, starting from a plane bed with n = 0.012. A quasi-uniform and quasi-steady regime was assumed to occur in each simulation step, with computed hydro-sedimentological parameters being deemed representative of channel reach conditions. These hypotheses and other aspects of the computation procedure were verified by Granadier (2020), where further explanation and simulation scenarios and results are also provided.

3 - RESULTS

Simulation results are shown in Table 1 at 2 hr intervals during ripple development (equilibrium occurred at time T = 32 hr in this transient flow simulation), and at 4 hr intervals thereafter until T = 72 hr (end of the flood hydrograph). Throughout the simulation, it can be noted that h (actual water depth), h_e and θ_e were positively correlated with q, while t_e was negatively correlated with q. Ripple dimensions, k_s and n values increased monotonically until the equilibrium stage was reached, then remained constant and equal to the corresponding equilibrium value. The gap between h and h_e values is attributed to taking ripple development into account *vis-à-vis* assuming equilibrium ripple dimensions (constant in time) as part of the roughness calculation procedure, as discussed further e.g. in Granadier and Rauen (2019) and

Granadier (2020). Normalised time and ripple dimensions computed from the results shown in Table 1 gave the exact same curves as illustrated in Figure 1a.

Table 1 also revealed a mismatch between the hydrograph time stamp (T) and the time stamps associated with the ripple development history (t_i and t_f). In the calculation procedure, equation (3) adjusts the ripple time as a function of instantaneous ripple dimensions, as if they had been reached under the instantaneous flow condition. This step effectively delayed ripple time in relation to hydrograph time as the discharge increased, while advancing it as the discharge decreased. Such an effect can be noted in Table 1 by comparing the t_f value of a given time step with the subsequent t_i value. For instance, during hydrograph ascension the ripple time decreased from t_f = 5.8 hr at T = 10 hr to t_i = 5.2 hr at T = 11 hr, while, in contrast, during hydrograph descent, the ripple time increased from t_f = 20.0 hr at T = 30 hr to t_i = 20.7 hr at T = 31 hr. In this simulation the equilibrium stage was reached at T = 32 hr, the hydrograph time step during which the ripple time reached the corresponding t_e value – when an overall ratio of t_e/T = 0.7 was obtained, for the particular set of hydro-sedimentological conditions. The fact that such a ratio is lower than unity suggests that, in net relative terms ripple development was accelerated by the flood wave, an effect which was probably caused by the early development stage from plane bed (when higher growth rates take place, see Figure 1b) occurring during hydrograph ascension.

Table 1 – Simulation results obtained for ripple development under transient flow.

T (hr)	q (m^3/sm)	h (m)	h_e (m)	θ_e	t_e (hr)	t_i (hr)	t_f (hr)	η_i (m)	η_f (m)	λ_i (m)	λ_f (m)	k_s (m)	n
0	0.11	0.36	0.54	0.069	293.6	0.0	0.0	0.000	0.000	0.000	0.000	0.0010	0.012
1	0.12	0.48	0.59	0.076	224.1	0.0	1.0	0.000	0.003	0.000	0.038	0.0068	0.017
2	0.14	0.53	0.64	0.082	177.3	0.8	1.8	0.003	0.004	0.038	0.046	0.0091	0.018
3	0.16	0.58	0.68	0.088	144.3	1.5	2.5	0.004	0.004	0.046	0.053	0.0109	0.018
4	0.18	0.63	0.73	0.094	120.0	2.0	3.0	0.004	0.005	0.053	0.058	0.0127	0.019
5	0.19	0.68	0.77	0.099	101.5	2.6	3.6	0.005	0.005	0.058	0.063	0.0143	0.019
6	0.21	0.72	0.81	0.105	87.2	3.1	4.1	0.005	0.006	0.063	0.068	0.0159	0.019
7	0.23	0.76	0.85	0.110	75.8	3.5	4.5	0.006	0.006	0.068	0.073	0.0174	0.020
8	0.25	0.81	0.89	0.115	66.5	4.0	5.0	0.006	0.007	0.073	0.077	0.0190	0.020
9	0.27	0.85	0.93	0.120	59.0	4.4	5.4	0.007	0.007	0.077	0.081	0.0205	0.020
10	0.28	0.89	0.96	0.124	52.6	4.8	5.8	0.007	0.008	0.081	0.085	0.0220	0.020
12	0.32	0.96	1.03	0.133	42.8	5.7	6.7	0.008	0.009	0.089	0.092	0.0251	0.021
14	0.35	1.04	1.10	0.142	35.6	6.4	7.4	0.009	0.009	0.096	0.099	0.0281	0.021
16	0.39	1.11	1.17	0.150	30.1	7.2	8.2	0.010	0.010	0.103	0.106	0.0311	0.022
18	0.43	1.18	1.23	0.159	25.9	8.0	9.0	0.011	0.011	0.110	0.113	0.0342	0.022
20	0.46	1.25	1.29	0.166	22.5	8.7	9.7	0.012	0.012	0.116	0.120	0.0372	0.022
22	0.50	1.32	1.35	0.174	19.8	9.5	10.5	0.012	0.013	0.123	0.126	0.0403	0.023
24	0.53	1.38	1.41	0.181	17.5	10.2	11.2	0.013	0.014	0.129	0.132	0.0434	0.023
26	0.51	1.36	1.38	0.178	18.6	13.0	14.0	0.014	0.014	0.135	0.137	0.0462	0.023
28	0.50	1.34	1.35	0.174	19.8	15.9	16.9	0.015	0.015	0.140	0.142	0.0485	0.023
30	0.48	1.32	1.32	0.170	21.1	19.0	20.0	0.015	0.016	0.144	0.146	0.0506	0.023
32	0.46	1.29	1.29	0.166	22.5	22.4	23.4	0.016	0.016	0.147	0.148	0.0516	0.023
36	0.43	1.23	1.23	0.159	---	---	---	0.016	0.016	0.148	0.148	0.0516	0.023
40	0.39	1.17	1.17	0.150	---	---	---	0.016	0.016	0.148	0.148	0.0516	0.023
44	0.35	1.10	1.10	0.142	---	---	---	0.016	0.016	0.148	0.148	0.0516	0.023
48	0.32	1.03	1.03	0.133	---	---	---	0.016	0.016	0.148	0.148	0.0516	0.023
52	0.28	0.96	0.96	0.124	---	---	---	0.016	0.016	0.148	0.148	0.0516	0.023
56	0.25	0.89	0.89	0.115	---	---	---	0.016	0.016	0.148	0.148	0.0516	0.023
60	0.21	0.81	0.81	0.105	---	---	---	0.016	0.016	0.148	0.148	0.0516	0.023
64	0.18	0.73	0.73	0.094	---	---	---	0.016	0.016	0.148	0.148	0.0516	0.023
68	0.14	0.64	0.64	0.082	---	---	---	0.016	0.016	0.148	0.148	0.0516	0.023
72	0.11	0.54	0.54	0.069	---	---	---	0.016	0.016	0.148	0.148	0.0516	0.023

4 - FINAL REMARKS

The procedure outlined in section 2 can also be applied to simulate conditions in which mega-ripples and dunes occur on the channel bed, provided that their equilibrium dimensions are linked to the water depth. Disconnecting bed form development history from hydrograph history is an essential element of such modelling procedure, so that its effects on the bed form development history become a key outcome of simulations thus conducted. Further research could investigate related processes, while time series data of bed form development under transient flows would be useful for calibration and validation of predictions, as well as for guiding further model development.

ACKNOWLEDGEMENT – The second author gratefully acknowledges a masters level scholarship received from CAPES Foundation – Brazil, via PPGERHA-UFPR.

REFERENCES

BRUNNER, G. W. (2010). *HEC-RAS 4.1 river analysis system: hydraulic reference manual*. US Army Corps of Engineers, Davis, 789 p.

BRUNNER, G. W. (2016). *HEC-RAS 5.0 river analysis system: hydraulic reference manual*. US Army Corps of Engineers, Davis, 546 p.

COLEMAN, S. E.; ZHANG, M. H.; CLUNIE, T. M. (2005). "*Sediment-wave development in subcritical water flow*". Journal of Hydraulic Engineering, 131(2), 106-111.

DELTARES (2014). *Delft3D-FLOW 3.15: user manual*. Deltares, Delft, 684 p.

GRANADIER, V. (2020). "*Leito vivo: caracterização do acoplamento entre rugosidade dinâmica do leito e parâmetros do escoamento fluvial*". Dissertação (Mestrado em Engenharia de Recursos Hídricos e Ambiental), Federal University of Parana (UFPR) (in preparation).

GRANADIER, V.; RAUEN, W. B. (2019). "*Importância relativa do desenvolvimento de pequenas dunas na modelagem hidrossedimentológica fluvial*" in Anais do XXIII Simpósio ABRHidro, Foz do Iguaçu, 2019, 1-10.

PAARLBERG, A. J.; DOHMEN-JANSSEN, C. M.; HULSCHER, S. J. M. H.; TERMES, P. (2009). "*Modeling river dune evolution using a parameterization of flow separation*". Journal of Geophysical Research, 114(1), 1-17.

RAUDKIVI, A. J. (1997). "*Ripples on stream bed*". Journal of Hydraulic Engineering, 123 (1), 58-64.

SOULSBY, R. (1997). *Dynamics of marine sands*. Thomas Telford, Londres, 253 p.

VAN RIJN, L. C. (2007). "*Unified view of sediment transport by currents and waves: initiation of motion, bed roughness and bedload transport*". Journal of Hydraulic Engineering, 133(6), 649-667.

WARMINK, J. J.; VAN DUIN, O. J. M.; NAQSHBAND, S. (2015). "Comparison of two bed form models to predict bed form roughness for flood modelling" in Proceedings of the 36th IAHR Congress, The Hague, 2015, 1-6.